Nanoscale

Accepted Manuscript

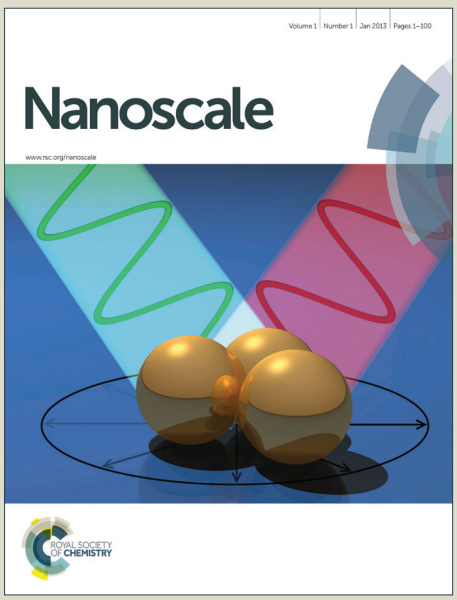

ROYAL SOCIETY OF CHEMISTRY

www.rsc.org/nanoscale

Phase Transition of a Perovskite Strongly Coupled to the Vacuum Field

Shaojun Wang,[a] Arkadiusz Mika,[a] James A. Hutchison,[a] Cyriaque Genet,[a] Abdelaziz Jouaiti,[b] Mir Wais Hosseini[b] and Thomas W. Ebbesen* [a]

The hysteresis and dynamics of the phase transition of the perovskite salt $[Pb(II)I_4^{2-}(C_{12}H_{25}NH_3^+)_2]$ is shown to be significantly modified when strongly coupled to the vacuum field inside a micro-cavity. The transition barrier is increased and the hysteresis loop is enlarged, demonstrating the potential of controlling the electromagnetic environment of a material.

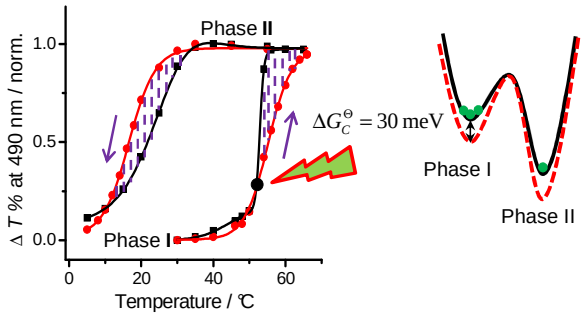

Hysteresis and energy barrier of a phase transition are shown to be significantly modified by strong coupling (red curves).

Hysteresis in phase transitions is a widely observed phenomenon in molecular and solid state systems in chemistry, biology and physics.[1-10] It is studied both for its fundamental features and its technological applications. Most notably, a stable hysteresis in phase-transition materials, such as polymer gels, spin-crossover complexes, charge-transfer materials and ferroelectric, form the basis for memory and data storage.[3-10] The hysteresis in molecular materials is very often dynamic, evolving in time depending on the barrier between the two phases in the transition. Great efforts have been spent to broaden and stabilize such hysteresis by chemical modification.[5-6] Here we demonstrate, for the first time, that such hysteresis can be also modified and stabilized by strong light-matter interactions.

Hysteresis always involves cooperative interactions and the formation of metastable states.[1,2] Light-matter strong coupling may also involve the collective interaction of a large number of oscillators N with a single optical resonance inside a cavity[11-19] such as that formed by two mirrors (Fabry-Perot cavity). As a consequence, coherent states[20] are generated which results in an enhanced Rabi splitting of magnitude $\hbar\Omega_{\mathrm{R}}^{\mathrm{N}} = \sqrt{\mathrm{N}} \cdot \hbar\Omega_{\mathrm{R}}$ where $\hbar\Omega_{\mathrm{R}}$ is the splitting that would be induced by a single oscillator. Two new hybrid light-matter states are formed, P+ and P- , as depicted in **Figure 1a**. The Rabi splitting depends on the transition dipole moment *d* of the oscillator and the electric field *E* in the cavity as given by **equation (1)** in the absence of dissipation:

$$\hbar\Omega_R = 2d \cdot E = 2d \cdot \sqrt{\frac{\hbar\omega}{2\varepsilon_0 v}} \cdot \sqrt{n_{ph} + 1} \qquad (1)$$

where $\hbar\omega$ is the cavity resonance or transition energy, ε_0 the vacuum permittivity, v the mode volume and n_{ph} the number of photons present in the system. Even when n_{ph} goes to zero, $\hbar\Omega_{\mathrm{R}}$ has a finite value due to the vacuum electromagnetic field. All the experiments reported here are in this limit. Nevertheless the Rabi splitting can be very large due to the large number N of oscillators and the small mode volume of micro-cavities if all the parameters are properly tuned.

The strong modification of the energy levels of a material due to light-matter hybridization has been shown to affect relaxation pathways in the coupled system[15-16,19], the rates of the photochemical reactions[16], and to tune the work-function of organic-semiconductors[17]. Our recent thermodynamic study demonstrated that the ground states also can be engineered under strong coupling regime.[18] An important number is the relative fraction $\hbar\Omega_{\mathrm{R}}^{\mathrm{N}} / \hbar\omega$ since it is an indication of the perturbation of the electronic structure of

the material and therefore the shift in the ground state energy $\Delta G_C^{\ominus}$ as illustrated in **Figure 1a**.[18] $\Delta G_C^{\ominus}$ is the change in the standard Gibbs free energy which determines the fraction of coupled molecules in the resonant cavity. In the so-called ultra-strong coupling regime $\hbar\Omega_R^N / \hbar\omega$ is typically > 0.1, conditions we will use in this study.

Perovskites such as the hybrid $[Pb(II)I_4^{2-},(C_{12}H_{25}NH_3^+)_2]$ ($PbI_4(R\text{-}NH_3)_2$) salt are known to undergo a phase transition near room temperature involving a bond angle change[21-24], as illustrated in **Figure 2a** and the corresponding spectra of phase I and phase II are given in **Figure 2c**. The sharp absorption peaks of the two phases are separated by 21 nm or 114 meV. The transition temperatures are ~ 50 °C upon warming and ~ 25 °C upon cooling (**Figure 2b**) which define the hysteresis loop to which we will return further down.

It has been shown that two dimensional layered perovskites can be strongly coupled to an optical resonance.[11,25-26] Here we achieve a higher $\hbar\Omega_R^N$, and thereby $\hbar\Omega_R^N / \hbar\omega$, by placing a 25 nm film of $PbI_4(R\text{-}NH_3)_2$ at the antinode of $\lambda / 2$ metallic Fabry-Perot cavity which is resonant with the absorption transition of the perovskite as schematically shown in **Figure 1b**. As we have reported elsewhere for another compound,[19] this gives a stronger coupling than if the same amount of material is evenly distributed in the cavity. Technically this was achieved by using a multilayer structure (**Figure 3a** and see Sample preparation). The transmission spectra of the cavity with and without the compound are shown in **Figure 2d**. Two new peaks, corresponding to P+ and P-, appear for both phases which are separated by an energy greater than the width of the cavity resonance (Q factor ~10-20) and the molecular absorption, the signature of strong coupling. In other words, phase I and II are both coupled to the same optical resonance at roughly the same strength. The angular optical dispersion shown in **Figure 2e** for phase I confirms the anti-crossing due to the Rabi splitting. $\hbar\Omega_R^N$ is found to be as large as ~ 320 meV due the location of $PbI_4(R\text{-}NH_3)_2$ at the maximum field amplitude *E* (**Equation (1)**). As a consequence $\hbar\Omega_R^N / \hbar\omega$ ~ 0.13 and this should be sufficient to perturb the phase transition which was then investigated. Note that the peak in the cavity transmission spectra at 326 nm (**Figure 2d**) is due to the bulk plasmon transparency of silver, which overlaps with higher absorption bands of the perovskite.

Figure 3 shows the hysteresis loops between phase I and II recorded optically as a function of temperature under different conditions. In order to avoid any variance associated with using different samples, the hysteresis loops were always recorded by

preparing samples simultaneously in the absence and presence of strong coupling. The mirrors were isolated from the $PbI_4(R\text{-}NH_3)_2$ by a PMMA layer to avoid any chemical interference. The compound was transferred by stamping a PDMS block on the bottom PMMA layer and then the top half of the cavity, consisting of PMMA/Ag mirror deposited on another PDMS block, was gently connected to the first half (the detail is explained by the sample preparation). In the non-cavity case, the top did not have the second Ag mirror as illustrated in **Figure 3a**.

The change in hysteresis induced by strong coupling can be seen in **Figure 3c** and **d** as recorded at 490 nm and 511 nm corresponding respectively to phase I and II. It is immediately apparent that the hysteresis has broadened by 25% and changed shape. For instance on going from phase II to I the onset temperature moves by 10 °C (from 30 to 20 °C in **Figure 3d**). The data is plotted as a variation in transmission and normalized to the two phases in order to be able to compare the data (see Experimental Methods). Note that we did not observe hysteresis broadening in off-resonance cavities, e.g. when $\lambda / 2$ cavity mode is shifted to 700 nm. The stabilisation of on-resonance cavity is further confirmed by looking at the time evolution of the hysteresis. The dynamics are significantly slowed under the strong coupling as shown in **Figure 4** where we compare the kinetics in and out of the cavity. The kinetics are multi-exponential due to the heterogeneity of the $PbI_4(R\text{-}NH_3)_2$ phases, nevertheless it is clear that the phase transition is much slower inside the cavity. The first half-life increases by a factor ~3 in the strongly coupled system as can be seen in **Figure 4a** and **c**, where the system reaches pure phase II at 52 °C within two hours. For the cooling data at 30 °C (**Figure 4b** and **d**), the kinetics are so slow that Phase I is not reached in reasonable times for the strongly coupled state.

These findings are completely consistent with the lowering of the ground state of the coupled perovskites. Thermodynamic studies[18] show that the ground state of strongly coupled molecules is lowered as the Rabi splitting increases, as predicted by second order perturbation theory[27]. Here both phases are strongly coupled by the same optical mode however the barrier between them is not coupled since the transient population on the barrier is always negligible. Therefore, only the minima in the potential curves of the phase I and II are lowered as illustrated in **Figure 2b** and the transition barrier increases. A change in barrier height of ~30 meV (2.9 kJ/mole) can be estimated from the ratio in the half-lifes upon strong coupling using a simple Arrhenius rate dependence

$(1/\tau_{1/2} \approx A\exp(-\Delta E/k_B T))$ and assuming the pre-exponential A-factor to be constant. In other words the ground states of the two perovskite phases are stabilized by this amount.

Although light-matter strong coupling is associated with splitting excited states, it can also be used to modify the ground state energy landscape such as demonstrated here for the first time in the case of a phase transition. Increasing the Rabi splitting will enhance such effects in two ways, first by the direct perturbation of the ground state and secondly by increasing the fraction of coupled oscillators in the cavity.[18] Here the optical resonances was provided by metallic cavities which have the benefit of having small mode volumes but variety of other structures are also possible depending on the application, such as propagating and localized surface plasmon resonances[28-35], and distributed feedback cavities[11]. These results demonstrate that a molecular phase transition can be engineered by controlling the electromagnetic environment provided by the vacuum field, with both fundamental and technological implications.

Experimental Methods

Perovskite synthesis: $[Pb(II)I_4^{2-},(C_{12}H_{25}NH_3^+)_2]$ was synthesized by a modified procedure inspired by a literature contribution.[21-23] PbI_2 was dissolved in a 2:1 acetonitrile: methanol solution at 60 °C. To the clear solution thus obtained, HI (57 wt.% in water) was added drop-wise. To the mixture, a stoichiometric amount of dodecylamine ($C_{12}H_{25}NH_2$) in a 2:1 acetonitrile: methanol was added. The mixture was further stirred at 60 °C for 1 hour. The desired $[Pb(II)I_4^{2-},(C_{12}H_{25}NH_3^+)_2]$ salt precipitated from solution upon slow evaporation of solvents. No further purification was necessary. All the inorganic, organic salts and solvents were commercially available by Sigma-Aldrich.

Sample preparation: We used a bonding technique[15,19,29] for the precise deposition of $[Pb(II)I_4^{2-},(C_{12}H_{25}NH_3^+)_2]$ films in the center of metallic micro-cavities. Briefly, a 30 nm-thick silver film was sputtered on a clean glass substrate, upon which was spin-coated a 40 nm film of poly(methyl methacrylate) (PMMA) (labeled slab A). Slab A was annealed at 70 °C on a hotplate for 15 minutes. A 25 nm thick $[Pb(II)I_4^{2-},(C_{12}H_{25}NH_3^+)_2]$ film was spun onto a separate block of poly(dimethylsiloxane) (PDMS), the surface of which had been rendered hydrophilic by oxygen plasma treatment. The $[Pb(II)I_4^{2-},(C_{12}H_{25}NH_3^+)_2]$film on the PDMS block was kept at 5 °C for 30 minutes. Then the dried film was transferred onto slab A by stamping the PDMS block. Meanwhile, a 30 nm-thick silver film and ~40 nm

layer of PMMA were successively deposited on another 1.0 mm thick PDMS substrate by electron evaporation and spin coating (labeled slab B). Slab B was annealed at 70 °C on a hotplate for 15 minutes. Then 0.3% by weight PDMS (poly(dimethylsiloxane), hydroxyl-terminated, MW = 110 000, Aldrich) dissolved in *tert*-butanol was spin cast at 6500 rpm on the slab B, forming a very thin layer (~ 2 nm) to increase adherence in the next step. Finally, the polymer face of slab B was gently pressed onto $[Pb(II)I_4^{2-},(C_{12}H_{25}NH_3^+)_2]$ surface of slab A to form a low Q factor cavity (~10-20). Simultaneously, a non-cavity sample was prepared by the same procedure without 30 nm silver film on slab B. This whole procedure with the two slabs was developed to avoid any possible perturbation of $[Pb(II)I_4^{2-},(C_{12}H_{25}NH_3^+)_2]$ and its phase transition properties.

***Measurements**:* Steady-state transmission and absorption spectra were taken on a Shimadzu UV3101 spectrometer throughout the range of 300 – 700 nm. The angular dispersion of transmission spectra were measured with an optical set-up. The temperature was controlled from 5 °C to 66 °C by a precise thermoregulation (Huber). Before recording a spectrum, temperature setting was kept as long as 5 minutes to ensure thermal equilibrium. Generally, phase transitions of molecular materials are measured by monitoring the change in absorbance (ΔA) as a function of temperature. Since we are dealing here with cavities, it is difficult to extract the absorbance from the Fabry-Perot transmission data without inducing additional errors. For this reason, the change of transmission ΔT%, normalized by the differential transmission of pure phase I and phase II, is plotted as a function of temperature. The error induced by ΔT as compared to ΔA is small because the values of ΔA are typically less than 0.1.

Acknowledgements

This work was supported in part by the ERC Plasmonics (GA-227557), the ANR Equipex "Union" (ANR-10-EQPX-52-01), the Labex NIE (ANR-11-LABX-0058_NIE) and USIAS within the Investissement d'Avenir program ANR-10-IDEX-0002-02. S.W. acknowledges the personal support from the Chinese Scholarship Council (CSC).

Notes and references

[a] *ISIS & icFRC, Université de Strasbourg and CNRS, 8 allée Monge, 67000 Strasbourg Cedex, France; E-mail: ebbesen@unistra.fr*

[b]*Laboratoire de Tectonique Moléculaire & icFRC, Université de Strasbourg and CNRS,Institut Le Bel, 4 rue Blaise Pascal, 67070 Strasbourg Cedex, France*

1. E. Neumann, *Angew. Chem. Int. Ed*. **1973**, *12*, 356.
2. D. R. Knittel, S. P. Pack, S. H. Lin and L. Eyring, *J. Chem. Phys.* **1977**, *67*, 134.
3. A. Suzuki and T. Tanaka, *Nature* **1990**, *346*, 345.
4. O. Kahn and C. J. Martinez, *Science* **1998**, *279*, 44.
5. R. Lopez, L. A. Boatner, T. E. Haynes, R. F. Haglund Jr. and L. C. Feldman, *Appl. Phys. Lett.* **2001**, *79*, 3161.
6. O. Sato, J. Tao and Y. Z. Zhang, *Angew. Chem. Int. Ed.* **2007**, *46*, 2152.
7. T. Driscoll, H. T. Kim, B. G. Chae, M. Di Ventra and D. N. Basov, *Appl. Phys. Lett.* **2009**, *95*, 043503.
8. T. Mahfoud, G. Molnár, S. Bonhommeau, S. Cobo, L. Salmon, P. Demont, H. Tokoro, S. I. Ohkoshi, K. Boukheddaden and A. Bousseksou, *J. Am. Chem. Soc.* **2009**, *131*, 15049.
9. S. I. Ohkoshi, Y. Tsunobuchi, T. Matsuda, K. Hashimoto, A. Namai, F. Hakoe and H. Tokoro, *Nature Chem.* **2010**, *2*, 539.
10. F. Kagawa, S. Horiuchi, N. Minami, S. Ishibashi, K. Kobayashi, R. Kumai, Y. Murakami and Y. Tokura, *Nano Lett.* **2014**, *14*, 239.
11. T. Fujita, Y. Sato, T. Kuitani and T. Ishihara, *Phys. Rev. B* **1998**, *57*, 12428.
12. D. G. Lidzey, D. D. C. Bradley, M. S. Skolnick, T. Virgili, S. Walker and D.M. Whittaker, *Nature* **1998**, *395*, 53.
13. P. A. Hobson, W. L. Barnes, D. G. Lidzey, G. A. Gehring, D. M. Whittaker, M. S. Skolnick and S. Walker, *Appl. Phys. Lett.* **2002**, *81*, 3519.
14. T. Schwartz, J. A. Hutchison, C. Genet and T. W. Ebbesen, *Phys. Rev. Lett.* **2011**, *106*, 196405.
15. J. A. Hutchison, T. Schwartz, C. Genet, E. Devaux and T. W. Ebbesen, *Angew. Chem. Int. Ed.* **2012**, *51*, 1.
16. T. Schwartz, J. A. Hutchison, J. Léonard, C. Genet, S. Haacke, and T. W. Ebbesen, *ChemPhysChem* **2013**, *14*, 125.
17. J. A. Hutchison, A. Liscio, T. Schwartz, A. C. Durand, C. Genet, V. Palermo, P. P. Samorì and T. W. Ebbesen, *Adv. Mater.* **2013**, *25*, 2481.
18. A. Canaguier-Durand, E. Devaux, J. George, Y. Pang, J. A. Hutchison, T. Schwartz, C. Genet, N. Wilhelms, J.-M. Lehn and T. W. Ebbesen, *Angew. Chem. Int. Ed.*, **2013**, *52*, 10533.

19. S. Wang, T. Chervy, J. George, J. A. Hutchison, C. Genet and T. W. Ebbesen, *J. Phys. Chem. Lett.*, **2014**, *5*, 1433.
20. "Cavity quantum electrodynamics": S. Haroche in Fundamental Systems in Quantum Optics (Eds.: J. Dalibard, J. M. Raimond, J.Zinn-Justin), Les Houches Summer School, Session LIII, Amsterdam, **1990**.
21. D. B. Mitzi. *Prog. Inorg. Chem.* **1999**, *48*, 1.
22. J. L. Knutson, J. D. Martin and D. B. Mitzi, *Inorg. Chem.* **2005,** *44*, 4699.
23. D. G. Billing and A. Lemmerer, *New J. Chem.* **2008**, *32*, 1736.
24. K. Pradeesh, J. J. Baumberg and G. V. Prakash, *Appl. Phys. Lett.* **2009**, *95*, 173305.
25. G. Lanty, A. Brehier, R. Parashkov, J. S. Lauret and E. Deleporte, *N. J. Phys.* **2008**, *10*, 065007.
26. K. Pradeesh, J. J. Baumberg and G. V. Prakash, *Opt. Express* **2009**, *17*, 22171.
27. C. Ciuti, G. Bastard and I. Carusotto, *Phys. Rev. B* **2005**, *72*, 115303.
28. J. Dintinger, S. Klein, F. Bustos, W.L. Barnes and T.W. Ebbesen, *Phys. Rev. B* **2005**, *71*, 035424.
29. T. K. Hakala, J. J. Toppari, A. Kuzyk, M. Pettersson, H. Tikkanen, H. Kunttu, and P. Törmä, *Phys. Rev. Lett.***2009**, *103*, 053602.
30. P. Vasa, R. Pomraenke, G. Cirmi, E. De Re, W. Wang, S. Schwieger, D. Leipold and C. Lienau, *Acs Nano* **2010**, *42*, 7559-7565.
31. A. Salomon, S. Wang, J. A. Hutchison, C. Genet and T. W. Ebbesen, *ChemPhysChem* **2013**, *14*, 1882.
32. W. Ni, Z. Yang, H. Chen, L. Li and J. Wang, *J. Am. Chem. Soc.* **2008**, *130*, 6692.
33. Y.-W. Hao, H.-Y. Wang, Y. Jiang, Q.-D. Chen, K. Ueno, W.-Q. Wang, H. Misawa and H.-B. Sun, *Angew. Chem. Int. Ed.* **2011**, *123*, 7970.
34. G. Zengin, G. Johansson, P. Johansson, T. J. Antosiewicz, M. Käll and T. Shegai, *Sci. Rep.* **2013**, doi:10.1038/srep03074
35. F. Nagasawa, M. Takase and K. Murakoshi, *J. Phys. Chem. Lett.* **2014**, *5*, 14.

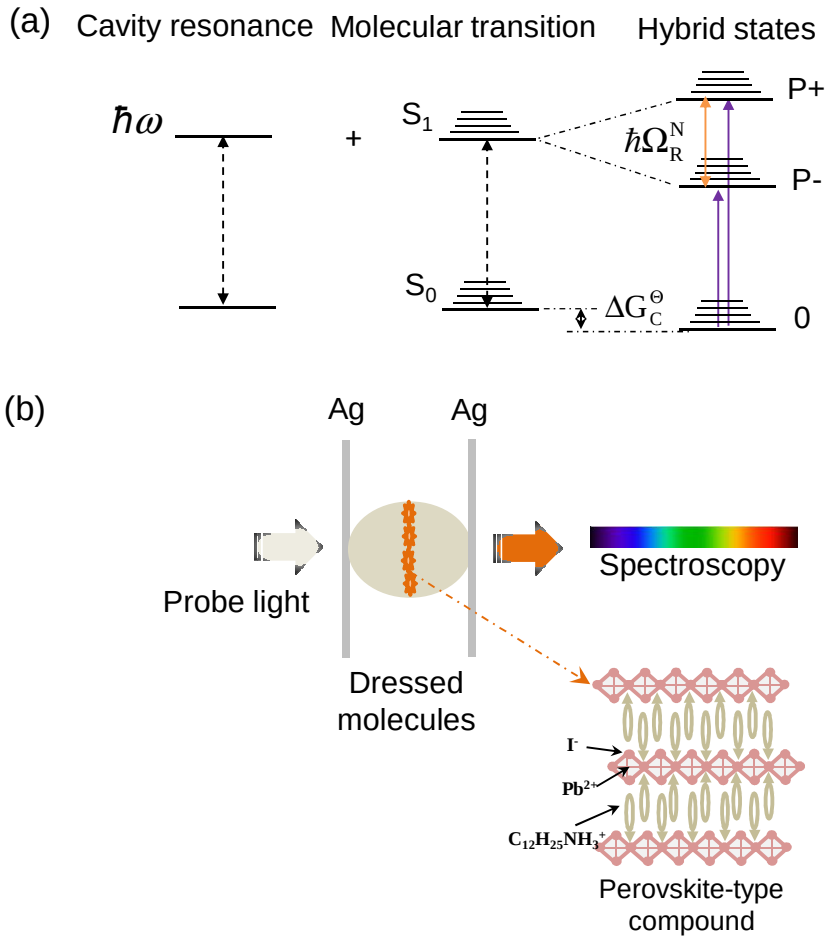

Figure 1. (a) The strong coupling between molecules resonant with a cavity mode $\hbar\omega$, generating two new eigen hybrid light-matter states P+ and P- separated by the Rabi-splitting energy $\hbar\Omega_R^N$. The ground-state energy of the coupled or dressed molecules is modified as compare to the bare molecules by the standard Gibbs free energy ΔG_C^Θ. (b) Schematic representation of two-dimensional layered perovskite $[Pb(II)I_4^{2-},(C_{12}H_{25}NH_3^+)_2]$ $(PbI_4(R\text{-}NH_3)_2)$ salt deposited at the anti-node of half-wavelength cavity. Optical spectroscopy was used to analysis $PbI_4(R\text{-}NH_3)_2$'s thermal phase transition property.

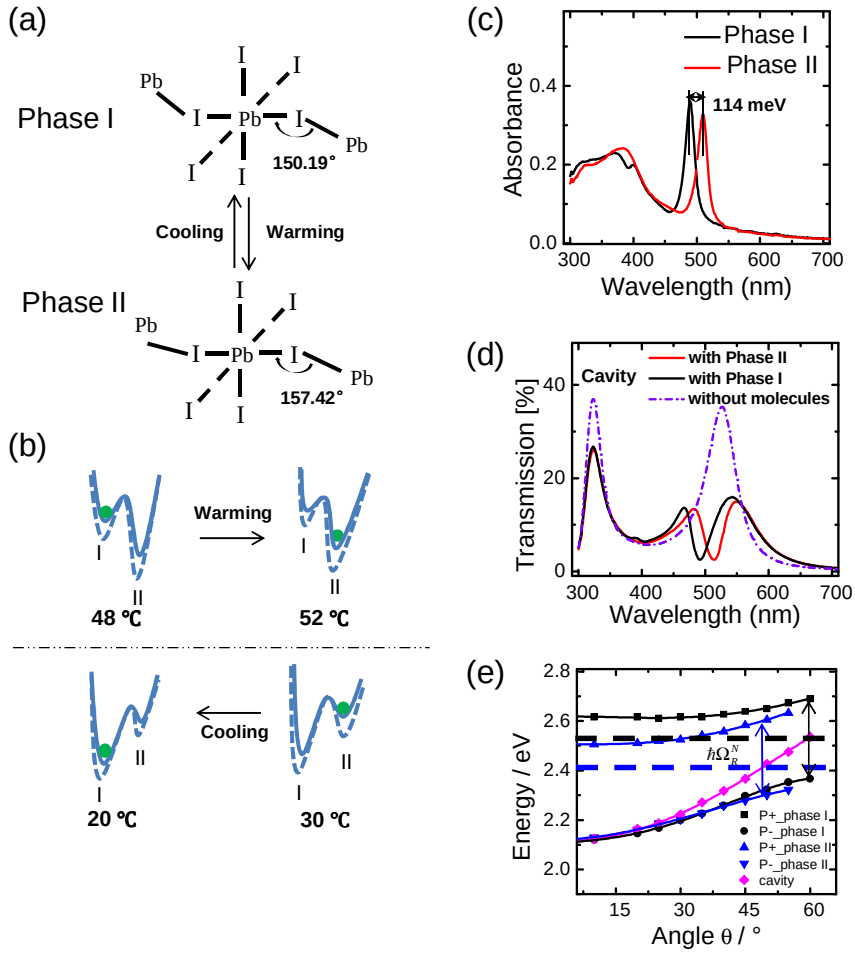

Figure 2. (a) $PbI_4(R\text{-}NH_3)_2$ bond angle change during the transition between phase I and II.[22-24] (b) Diagram of the Gibbs free energy with minima corresponding to states in phase I and II at different temperatures in the hysteresis. The dotted lines indicated ground state shift due to strong coupling. (c) The ground state absorption spectra of bare $PbI_4(R\text{-}NH_3)_2$ film in phase I and II, separated by 21 nm (114 meV). (d) Transmission spectra of cavity alone and with $PbI_4(R\text{-}NH_3)_2$ in phase I and II. (e) Angular dispersion of the cavity with $PbI_4(R\text{-}NH_3)_2$ in phase I (and II), the absorption peak of which is indicated by black (and blue) dashed line. In both cases, $\hbar\Omega_R^N$ is ~ 320 meV.

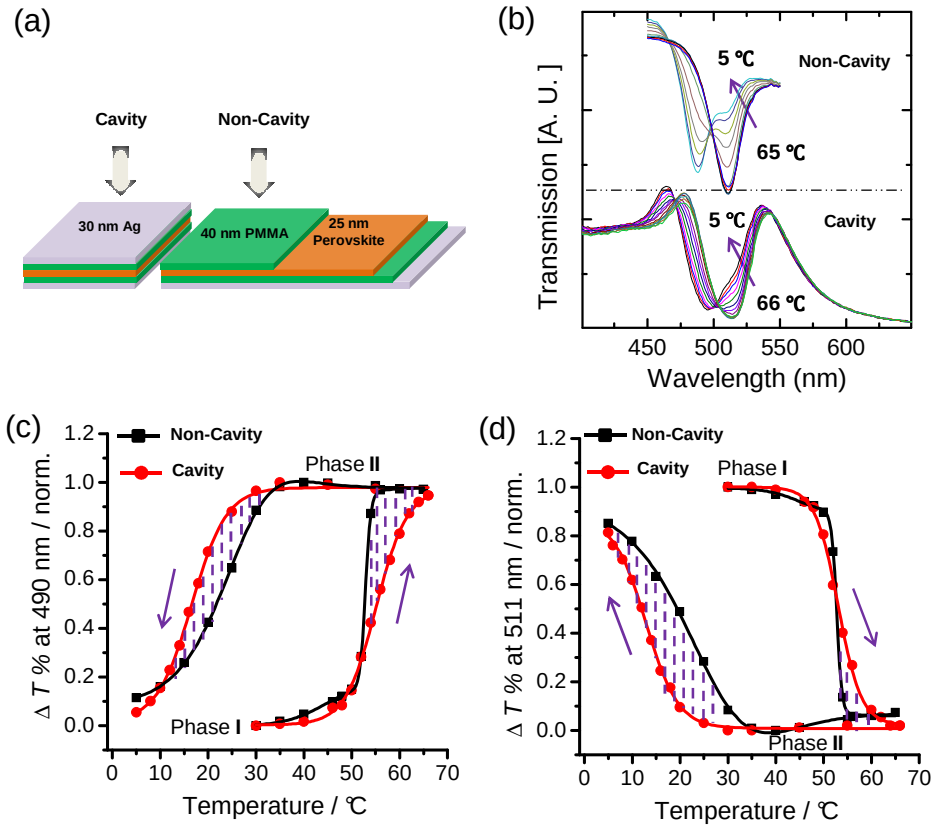

Figure 3. (a) The structure of cavity and its reference (non-cavity). Note that the two samples were made simultaneously by the same procedure, only difference being the presence of the top mirror in the cavity. (b) Examples of the evolution of transmission spectrum of the cavity and non-cavity as a function of temperature. (c) and (d) Graph of ΔT % (transmission intensity change at 490 nm (c) and 511 nm (d)) versus temperature for $PbI_4(R\text{-}NH_3)_2$ in cavity and non-cavity, the arrows show the direction of the temperature change. The dashed zones mark the enlargement of the hysteresis loop in the coupled system.

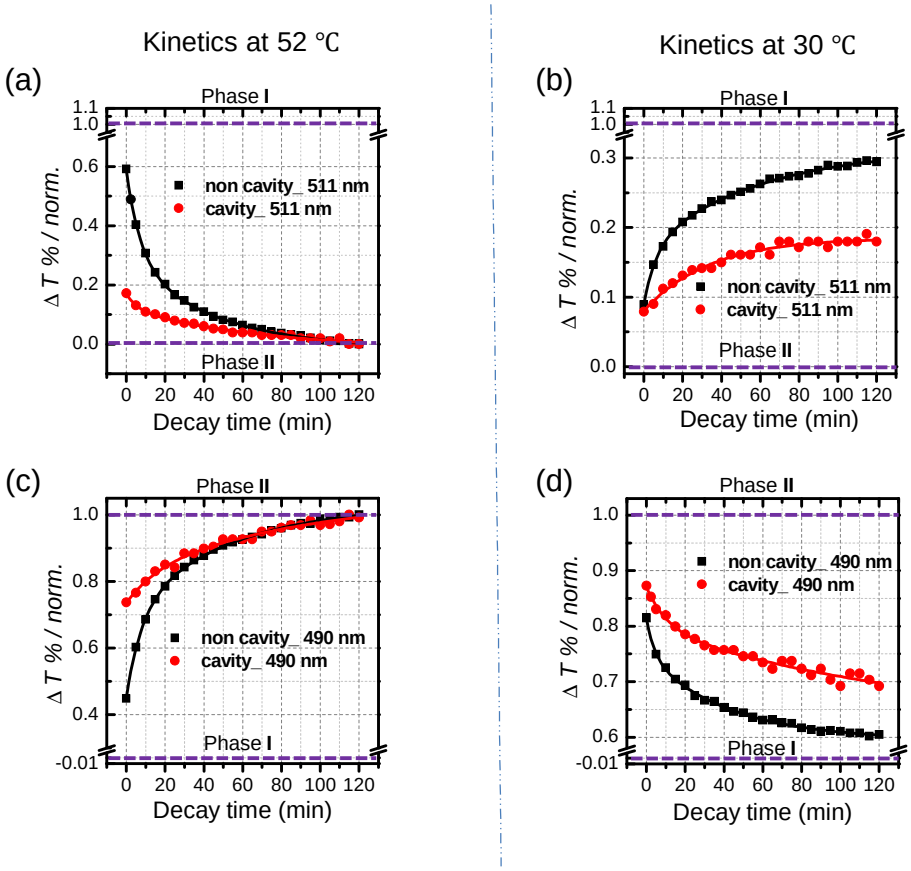

Figure 4. Kinetics of the evolution between phase I and II (indicated by violet dashed line) at 52 °C (a) and (c) in the warming cycle and at 30°C (b) and (d) in the cooling cycle, monitored by transmission intensity change at 490 nm for (c) and (d) and at 511 nm for (a) and (b).